The Adsorption of Tetramethylurea at the Mercury/Water Interface

Osamu IKEDA,* Hiroyuki JIMBO, and Hideo TAMURA

Department of Applied Chemistry, Faculty of Engineering, Osaka University, 2-1 Yamadaoka, Suita, Osaka 565

(Received June 1, 1982)

The adsorption of tetramethylurea (TMU) at the mercury/water interface was studied by means of differential capacity measurements. TMU was found to take three different orientations, depending on the surface excess and the charge sign of the electrode. These orientations could not be explained simply by the orientation of the TMU dipole in the electric field or by the hydrophobic interaction between the methyl groups of TMU and the electrode, but it was explained on the basis of interactions between TMU and water molecules, and on the basis of the TMU molecules themselves in the adsorption layer and an electronic polarization effect of the nitrogen atoms in TMU. A few water-adsorption models were compared in an attempt to estimate the dipole moment of the TMU molecule at the interface.

It has been shown in a recent paper[1] that tetramethylthiourea (TMTU) at the mercury/aqueous solution interface takes a vertical orientation with the sulfur atom on the electrode, in a manner similar to thiourea.[2] Such an orientation was explained on the basis of the hydrophobicity of the sulfur atom and the high electronic polarizability of the >C=S bond. In order to make these points clearer, it is desirable to study the adsorption behavior of tetramethylurea (TMU), in which the sulfur atom of tetramethylthiourea (TMTU) is displaced by the oxygen atom with a lower electronic polarizability and a higher hydrophilicity, compared to that of the sulfur atom. It is also interesting to see how the dipole moment of TMU, lower than those of other ureas,[3] is reflected in the adsorption behavior.

The adsorption behavior of organic compounds at the mercury/aqueous solution interface[4] is usually elucidated by a determination of the adsorption isotherm and by the change in the potential drop across the inner layer, $\Delta_2^M\phi$, due to adsorption. In the case of organic compounds with a polar group, a somewhat accurate orientation can be estimated from the change in $\Delta_2^M\phi$ due to adsorption. It has seldom been tried, however, to estimate the dipole moment of an adsorbed molecule because of the uncertainty in the potential drop due to adsorbed water dipoles, $\Delta g^w_{\text{dipole}}$. Parsons and his co-workers[5] first evaluated the dipole moment of an urea molecule at the mercury/water interface after the establishment of the water-adsorption model.[6] Studies along this direction seem to be important for a better understanding of the double-layer structure and property, and of their effects on the electrode kinetics.

The accurate evaluation of the dipole moment of an adsorbed molecule demands an accurate $\Delta g^w_{\text{dipole}}$ as a function of the electric field. Several water-adsorption models[7] have been proposed, along with $\Delta g^w_{\text{dipole}}$ as a function of the surface charge density. Aside from the idea contained in each model, however, the agreement in the values of $\Delta g^w_{\text{dipole}}$ is not so good among models. In this study, the Bockris-Habib (B-H) model,[8] the "experimental" model by Trasatti (T-model),[9] and the Damaskin-Frumkin (D-F) model[10] were taken up and compared in the evaluation of the dipole moment of an adsorbed TMU molecule.

Experimental

An analytical reagent grade of tetramethylurea (TMU) was used, it was vacuum-distilled twice before use. The sodium fluoride was of a high-purity reagent grade (Merck, ultrapure) and was used without further purification. The water and mercury were triply distilled before use. Nitrogen deoxygenated by passing it through copper meshes heated to 400 °C was used for deaeration and then blown over the solution. An aqueous 0.5 M NaF solution (1 M=1 mol dm^{-3}) was used as the supporting electrolyte. Eleven different concentrations of TMU were prepared to cover 2×10^{-3} M and 1×10^{-1} M.

The differential capacity, C, was measured at 25±0.1 °C using a dropping mercury electrode and by a method similar to that of Hills and Payne.[11] The measurement was carried out at 7.2 s after the birth of a mercury drop whose total life was about 13 s in pure 0.5 M NaF and at several frequencies, f, with an amplitude of 5 mV. The equilibrium capacities were obtained by extrapolating the linear relation of C against $f^{1/2}$ at a constant potential to $f=0$. A vertical capillary as the test electrode was prepared by drawing a Pyrex glass tube and was siliconed on the internal wall by passing through a vapor of dimethyldichlorosilane for several seconds. A KCl-saturated calomel electrode (SCE) and a cylindrical platinum plate, with a mercury drop at the center, were used as the reference and the counter electrode respectively. The mercury height from the reservior to the capillary tip was 1.4 m. The flow rate of mercury was determined by weighing mercury recovered during a given time.

The potential of zero charge, E_z was measured using a streaming electrode,[12] while the interfacial tension at the E_z, γ_z was measured by the maximum bubble pressure method following Schiffrin.[13] Most of the parameters essential to the analysis of the adsorption were derived by the double integration of the equilibrium capacity-potential curves using a computer program.

No corrections for the medium effects[14,15] on the activity of the supporting electrolyte or for the activity coefficient of the adsorbate[16] were taken into consideration.

Results and Discussion

Differential Capacity-potential Curves. Figure 1 shows the equilibrium differential capacity-potential curves measured with several concentrations of TMU. Two adsorption-desorption peaks are observed, but the shape of the peak at more negative potentials becomes higher and narrower than that at more positive po-

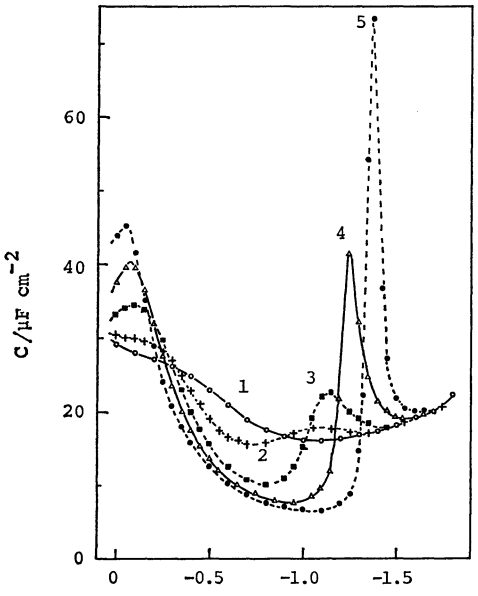

Fig. 1. Differential capacity-potential curves (extrapolated to zero frequency) of the mercury electrode in 0.5 M aqueous NaF solutions containing TMU at 25 °C.
Concentration of TMU (mM): (1) 0 (base solution, 0.5 M NaF), (2) 5, (3) 20, (4) 50, and (5) 100.

TABLE 1. DATA OF E_z AND γ_z

C_{TMU} / mol l^{-1}	E_z vs. SCE / V	γ_z / mN m^{-1}
0 (0.5 M NaF)	−0.432	426.8
0.002	−0.418	426.3
0.003	−0.412	426.0
0.005	−0.401	425·3
0.007	−0.392	424.8
0.010	−0.379	423.5
0.015	−0.362	422.4
0.020	−0.347	421.4
0.030	−0.324	419.5
0.050	−0.296	416.6
0.070	−0.278	414.4
0.100	−0.259	412.2

tentials with an increase in the concentration of TMU. This suggests that the attractive interaction among adsorbed molecules at more negative potentials is stronger than that at more positive potentials.[17]

Data of E_z and γ_z. Table 1 summarizes the data of E_z and γ_z. Positive shift of E_z with an increase in the concentration of TMU, C_{TMU}, was observed, as opposed to the negative shift of E_z in TMTU.[1] The orientation of TMU at E_z is expected to differ from that of TMTU.

Surface Excess. The surface excess, Γ, at a constant charge density, σ, was evaluated by means of the following relation: $\Gamma=-(1/RT)(\partial\xi/\partial\ln C_{TMU})$, where ξ is the Parsons function ($\xi=\gamma+\sigma E$).[18]

Figure 2 shows the variation in Γ at different concentrations of TMU with the surface charge density. The maximum of surface excess, Γ_{max}, was shifted toward a negative charge density with an increase in the concentration.

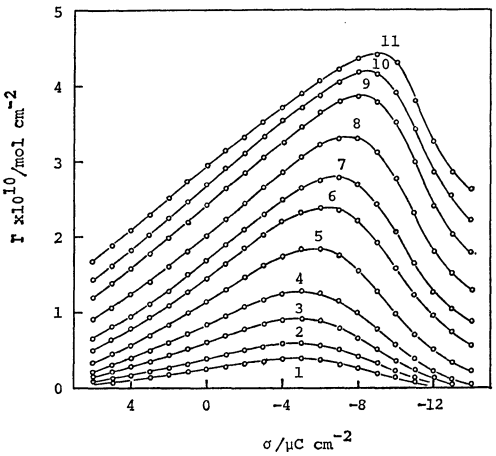

Fig. 2. Variation of surface excess of TMU with charge density at various concentrations.
Concentration of TMU (mM): (1) 2, (2) 3, (3), 5, (4) 7, (5) 10, (6) 15, (7) 20, (8) 30, (9) 50, (10) 70, and (11) 100.

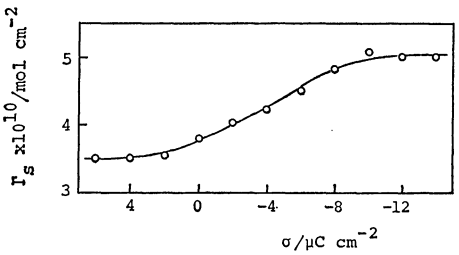

Fig. 3. Variation of Γ_s with surface charge density.

Figure 3 shows the surface excess at saturation, Γ_s, which was obtained by an extrapolation of the plot of $1/\Gamma$ against $1/C_{TMU}$ at a constant charge density to $1/C_{CMU}=0$. We observed two extreme values of Γ_s, namely, 3.5×10^{-10} mol dm^{-2} and 5.0×10^{-10} mol cm^{-2}, at positive and negative extremes of the surface charge density respectively.

Potential Drop across the Inner Layer, $\Delta_2^M\phi$. The value of $\Delta_2^M\phi$ was evaluated using this relation; $\Delta_2^M\phi=E-E_z-\Delta_S^2\phi$, where E and E_z are the potential at a constant charge density and the potential of zero charge for the electrolyte solution without any specific adsorption of ions (−0.432 V *vs.* SCE,[19]) respectively, and where $\Delta_S^2\phi$ is the potential drop across the diffuse layer at a constant charge density, which was calculated using the Gouy-Chapman theory.[20] The $\Delta_2^M\phi$ defined above corresponds to Grahame's rational potential difference.[20]

Figure 4 shows the change in $\Delta_2^M\phi$ due to the adsorption of TMU. The relations between $\Delta_2^M\phi$ and Γ for $\sigma\geqslant2$ μC cm^{-2} were linear, while those for $\sigma<2$ μC cm^{-2} were also linear at a lower surface excess, but were curved at a higher surface excess. When an adsorption isotherm can be described by the two series capacitor (TSC) model,[21] where the free energy

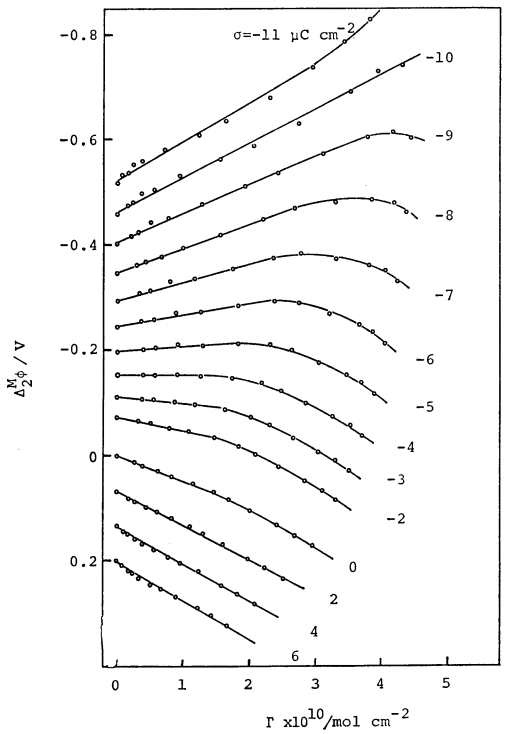

Fig. 4. Change in the potential drop across the inner layer due to adsorption of TMU.
Charge density is indicated by each line.

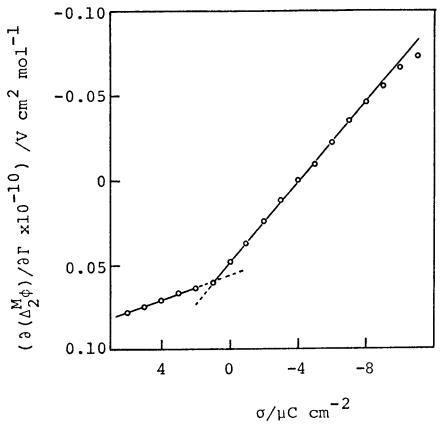

Fig. 5. Relation between $\partial(\Delta_2^M\phi)/\partial\Gamma$ obtained for the region where linear $\Delta_2^M\phi$-Γ relations were observed in Fig. 4 and the surface charge density.

of adsorption is a function of the charge density, a linear relation between $\Delta_2^M\phi$ and Γ should be observed for a constant orientation. In this sense, the linear portion of the $\Delta_2^M\phi-\Gamma$ curves in Fig. 4 can be assumed to result from a constant orientation based on the TSC model.

The magnitude of the positive shift of $\Delta_2^M\phi_{\sigma=0}$ with Γ for TMU is much larger than that of pyrazine[22] or ethylene glycol,[23] which are known as compounds with a small effective normal dipole moment, which means that the normal component of the dipole moment to the electrode surface is small. This suggests that TMU at a higher surface excess is adsorbed through an orientation with the positive end of the dipole toward the electrode surface.

Figure 5 shows the relation between the slope of the linear portion of the $\Delta_2^M\phi-\Gamma$ curves in Fig. 4 and the surface charge density. Two straight lines with different slopes are observed in Fig. 5. This indicates that the adsorption of TMU for $\sigma<2$ μC cm^{-2} and that for $\sigma\geqslant 2$ μC cm^{-2} can not be described by the same isotherm. Since the charge of the maximum adsorption, σ_{max}, is defined as σ at $(\partial\Delta_2^M\phi/\partial\Gamma)=0$,[4] the former is the adsorption with $\sigma_{max}=-15$——17 μC cm^{-2}, which was elucidated by an extrapolation, and the slope, $\partial(\partial\Delta_2^M\phi/\partial\Gamma)/\partial\sigma=3.87\times10^{10}$ mV cm^4 μC^{-1} mol^{-1}, while the latter is the adsorption with $\sigma_{max}=-4$ μC cm^{-2} and the slope of 11.83×10^{10} mV cm^4 μC^{-1} mol^{-1}.

Adsorption Isotherm and Free Energy of Adsorption. In order to determine the adsorption isotherm of TMU, various adsorption isotherms were examined using Γ in the region where linear portions were observed on the $\Delta_2^M\phi-\Gamma$ curves in Fig. 4; it was found that the adsorption of TMU could be described by the Frumkin isotherm:

$$\beta x = [\theta/(1-\theta)]\exp(-2\alpha\theta), \quad (1)$$

where β is the adsorption coefficient defined by $\exp(-\Delta\bar{G}^\circ/RT)$ containing the free energy of adsorption at zero coverage, $\Delta\bar{G}^\circ$, x is the molar fraction of the adsorbate, θ is the coverage, and α is the interaction parameter.

The Frumkin isotherm plot in Fig. 6 is drawn with respect to the regions where the linear $\Delta_2^M\phi-\Gamma$ relations were observed in Fig. 4, namely, $\sigma=-10$ μC cm^{-2} and $\sigma\geqslant 2$ μC cm^{-2}. The coverage was evaluated using Γ_s in Fig. 3; that is, $\Gamma_s=5.0\times10^{-10}$ mol cm^{-2} for $\sigma=-10$ μC cm^{-2} and $\Gamma_s=3.5\times10^{-10}$ mol cm^{-2} for $\sigma\geqslant 2$ μC cm^{-2}. It is thought from Fig. 6 that the adsorption of TMU in $\sigma\geqslant 2$ μC cm^{-2} can be described by the Frumkin isotherm with $\Gamma_s=3.5\times10^{-10}$ mol cm^{-2} and $\alpha=-0.25$. The deviation of the points at a lower coverage from a linear relation may be affected by a different adsorption, which will be discussed later. On the other hand, the adsorption of TMU at $\sigma=-10$ μC cm^{-2} could not be described

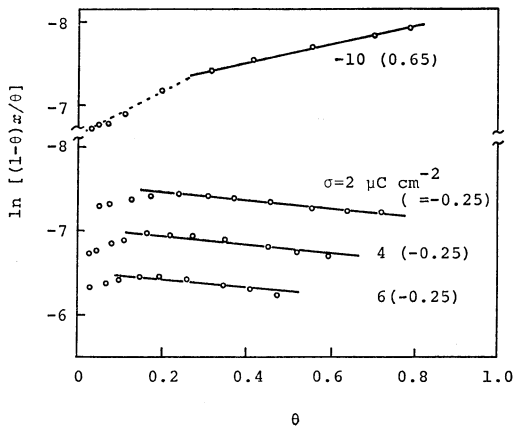

Fig. 6. Test of the Frumkin isotherm with Γ_s varing with surface charge density.
Charge density is indicated by each line, and the values in the parentheses represent the interaction parameter, α.

by a single isotherm throughout the coverage. The linear $\Delta_2^M\phi - \Gamma$ relation at $\sigma = -10\ \mu C\ cm^{-2}$ in Fig. 4 seems to be an incidental result. Probably, a change in the orientation or a mixed adsorption occurs with an increase in the surface excess at this charge density.

At a higher surface excess, the interaction parameter, which is shown in the parentheses of Fig. 6, was negative for $\sigma \geqslant 2\ \mu C\ cm^{-2}$, but was positive at $\sigma = -10\ \mu C\ cm^{-2}$. This difference in α at positive and far negative charges is compatible with the explanations given for the adsorption-desorption peaks in Fig. 1.

On the other hand, at a lower coverage in $\sigma < 2\ \mu C\ cm^{-2}$, the Γ_s seems to be different from the Γ_s shown in Fig. 3, because the latter is obtained by weighing the data at a higher surface excess. In order to estimate the Γ_s for a lower coverage, the following equation was used:[28]

$$\partial(\Delta_2^M\phi)/\partial\Gamma = -RT[\partial \ln \beta/\partial(\sigma - \sigma_{max})], \quad (2)$$

with a previously verified precondition that β is a function of the charge density. If a quadratic dependence of $\ln \beta$ on the charge density is assumed, Eq. 2 can be rearranged to Eq. 3:

$$\partial[\partial(\Delta_2^M\phi)/\partial\Gamma]/\partial(\sigma - \sigma_{max}) = -2RT[\partial \ln \beta/\partial(\sigma - \sigma_{max})^2]. \quad (3)$$

The left-hand side of Eq. 3 has already been estimated as the experimental slope for $\sigma < 2\ \mu C\ cm^{-2}$ in Fig. 5. Therefore, several Γ_s values were chosen and varied step-by-step until the $\ln \beta$ values obtained satisfy Eq. 3. The final value of Γ_s estimated in this way was $3.4—3.5 \times 10^{-10}$ mol cm^{-2}; the average was used in the subsequent analysis. Figures 7 and 8 show the Frumkin isotherm plot using the Γ_s finally estimated and the relation between $\ln \beta$ and $(\sigma - \sigma_{max})^2$ respectively. The satisfactory result with respect to Eq. 3 indicates that the assumption of the quadratic

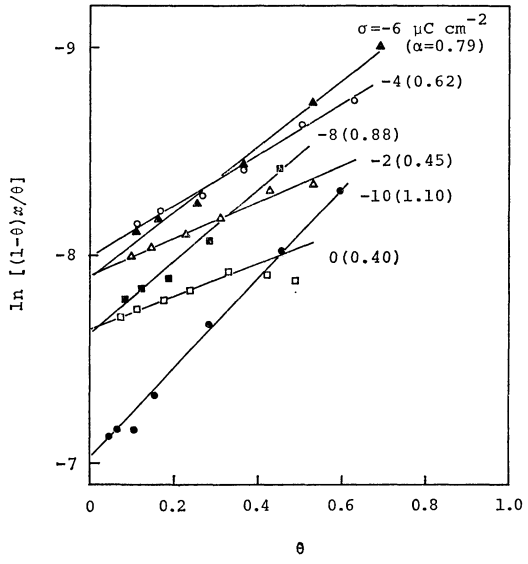

Fig. 7. The Frumkin isotherm plot using a constant $\Gamma_s = 3.45 \times 10^{-10}$ mol cm^{-2}.
Charge density is indicated by each line, and the values in the parentheses represent the interaction parameter, α.

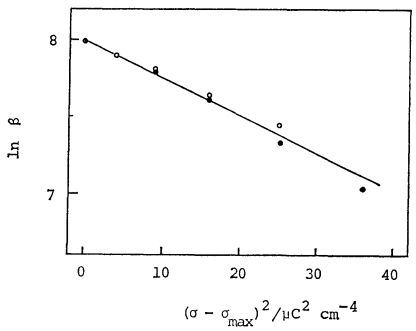

Fig. 8. Test of a quadratic dependence of $\ln \beta$ on the surface charge density.
Here open and closed circles correspond to $\ln \beta$ for $\sigma > \sigma_{max}$, and $\sigma < \sigma_{max}$ ($\sigma_{max} = -4\ \mu C\ cm^{-2}$), respectively.

dependence of $\ln \beta$ on the charge density and the estimated value of Γ_s are generally reasonable. The value of α shown in the parentheses of Fig. 7 were always positive, but changed with the surface charge density. According to the view of Pulidori and his co-workers,[27] the observed lowering of the positive α with an increase in the surface charge density means that the attractive interaction between TMU and water molecules becomes stronger, or that the attractive interaction among TMU molecules themselves becomes weaker with an increase in the surface charge density. So long as a constant orientation is assumed for the adsorption at a lower coverage, the fact that the attractive interaction varies with the charge density on the electrode suggests that adsorbed TMU molecules interact with the neighboring water structure, which also varies with the charge density.

Orientation Models of TMU. The following three fundamental orientations can be considered on the basis of the results presented thus far: (I) Orientation at a lower coverage in the region of $\sigma < 2\ \mu C\ cm^{-2}$. This orientation takes $\Gamma_s = 3.45 \times 10^{-10}$ mol cm^{-2} and $\sigma_{max} = -4.0\ \mu C\ cm^{-2}$, which suggests an orientation with a small effective normal dipole moment,[23] and it has positive interaction parameter. This will be a horizontal orientation where the >C=O group is approximately parallel to the electrode surface. (II) Orientation in the region of $\sigma \geqslant 2\ \mu C\ cm^{-2}$. This orientation takes $\Gamma_s = 3.5 \times 10^{-10}$ mol cm^{-2} and $\sigma_{max} = -15——17\ \mu C\ cm^{-2}$, which suggests an orientation with a large positive effective normal dipole moment, and it has negative interaction parameter. This will be a vertical orientation where the >C=O group is approximately vertical to the electrode surface. (III) Orientation at a higher coverage in the region of very negative charges. This orientation takes $\Gamma_s = 5.0 \times 10^{-10}$ mol cm^{-2} and has a positive interaction parameter because of lateral attractive interaction among the TMU dipoles in the adsorption layer.[26] This will also be a horizontal orientation where the >C=O group is nearly parallel to the electrode surface, but the occupied area is different from that of the (I) orientation.

The molecular structure of TMU, unlike that of urea,[27] has been considered to be non-planar because

of a steric repulsion. The single NMR signal of the CH_3 proton of TMU[28] is attributed to an internal rotation of the two $(CH_3)_2N-$ groups, which relieve the steric repulsion. In spite of its similar molecular structure[29] and the internal rotation property,[30] the dipole moment of TMU,[3] 11.6×10^{-30} C m, is greatly different from that of TMTU,[31] 15.7×10^{-30} C m. The dipole moment of TMU is smaller than that of urea,[3] 15.2×10^{-30} C m, but is rather close to that of acetone,[32] 9.7×10^{-30} C m. The lower dipole moment of TMU compared with that of TMTU may be attributable to a slightly deeper pyramidal structure of TMU about N atoms.[29] The most simple and unambiguous explanation, however, is a minor contribution of the conjugate system of $^+N{=}C{-}O^-$ to the dipole moment of TMU.[33] This leads to a consideration that the possibility of the distribution of a positive charge on N atoms is small.

In considering the orientation of TMU on the electrode, three possible extreme molecular conformations[30] were taken into account, and the average was taken for the projected area. Figure 9 shows the models corresponding to the three orientations, (I), (II), and (III). The projected areas of the rectangles enclosing a molecule were (I) 0.481, (II) 0.474, and (III) 0.332 nm^2, while the corresponding Γ_s values were (I) 3.45, (II) 3.5, and (III) 5.0×10^{-10} mol cm^{-2}. The averages of the molecular height, X_1, were estimated to be (I) 0.58, (II) 0.58, and (III) 0.62 nm.

Evaluation of the Dipole Moment of the TMU Molecule at the Interface. From the evaluation of the dipole moment of TMU adsorbed at the interface, we next attempted to confirm the three orientation models and to verify that the variation in the interaction parameter attributable to the charge density with respect to the (I) orientation is caused by the interaction with the neighboring water structure, not by a slight change in the orientation which leads to a change in the lateral attractive interaction among TMU dipoles.

The orientation of organic compounds with a polar group can be determined by the evaluation of the dipole moment of an adsorbed molecule using the following equation, which is similar to that derived by Parsons and his co-workers,[5] and by Damaskin and Frumkin:[34]

$$\Delta(\Delta_2^M\phi) = \theta[(\Gamma_s P_1/\varepsilon_1 - \Gamma_s n P_0/\varepsilon_0) + \sigma(1/K_1^i - 1/K_0^i)], \quad (4)$$

where ε, P, and K^i are the permittivity of the inner layer, the dipole moment of an adsorbed molecule, and the integral inner-layer capacity respectively, where n is the number of water molecules displaced by an adsorbate molecule, and where the subscripts 1 and 0 denote the inner layers saturated with adsorbate and water respectively.

The term $-\Gamma_s nP_0/\varepsilon_0$ in Eq. 4 is equal to the potential drop across the inner layer due to water dipoles, Δg^w_{dipole}. In the evaluation of the dipole moment of TMU, one can use several water-adsorption models[7] in which the value of Δg^w_{dipole} is given as a function of the charge density. The Bockris and Habib model was used in this study for the comparison of the results of TMU with those of TMTU.[1] In addition, the T-model[9] and the D-F model[10] were also applied to Eq. 4; the results will be compared below with those from the B-H model.

The integral inner-layer capacity in Eq. 4 should be $K^{i(ion)}$ as a result of free charges on the electrode; it is free from any contribution by dipoles, $K^{i(dipole)}$.[38] When the B-H model was applied to Eq. 4, $K_0^{i(ion)}$ was evaluated by substituting the K_0^i determined ex-

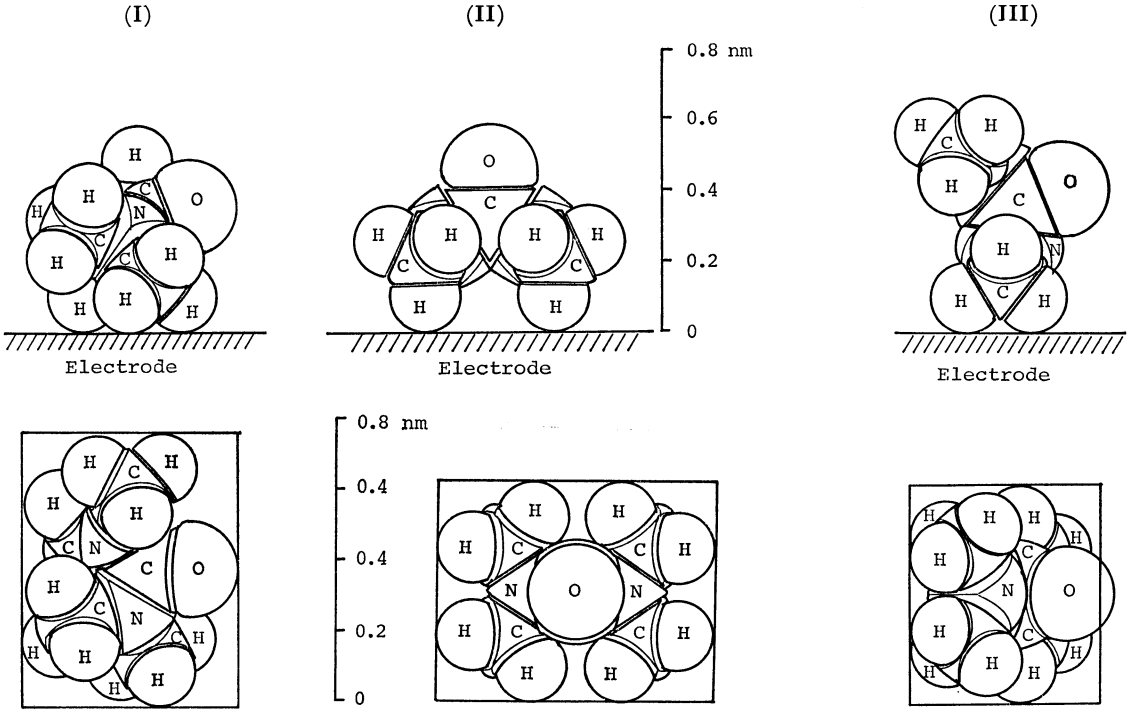

Fig. 9. Scale drawings of an adsorbed TMU molecule through the orientations, (I), (II), and (III). Upper and lower figures show the side and the top views, repectively. Rectangle enclosing a molecule means the projected area.

perimentally and the $1/K_0^{i(\text{dipole})}=8.0\times10^{-3}$ cm^2 μF^{-1} from the B-H model into this relation: $1/K_0^i=1/K_0^{i(\text{ion})}-1/K_0^{i(\text{dipole})}$. When the T and D-F models are applied to Eq. 4, the constant $K_0^{i(\text{ion})}$ values, 17 and 16 μF cm^{-2}, specified by each model were used. On the other hand, $K_1^{i(\text{ion})}$ was assumed to be equal to K_1^i.

For the evaluation of P_1 using Eq. 4, it is further necessary to estimate K_1^i and ε_1 as functions of the charge density. The values of K_1^i were obtained by plotting first the integral inner layer capacity at different surface excesses, K^i, against Γ, and then by extrapolating the plot to each Γ_s, as is shown in Fig. 10. The values of K_1^i for the (I) orientation were, however, obtained by extrapolating a linear relation between $1/K^i$ and Γ at each charge density to $\Gamma_s=3.45\times10^{-10}$ mol cm^{-2}. The values of ε_1 were calculated by substituting K_1^i and the molecular height, X_1, into this relation; $\varepsilon_1=X_1\cdot K_1^i$. Regarding orientations at full coverage in the region of $0\geqslant\sigma\geqslant-10$ μC cm^{-2}, X_1 was estimated by assuming a weighted average between the (II) orientation with $\Gamma_s=3.5\times10^{-10}$ mol cm^{-2} and $X_1=0.58$ nm, and the (III) orientation with $\Gamma_s=5.0\times10^{-10}$ mol cm^{-2} and $X_1=0.62$ nm, for the measured Γ_s in Fig. 3. The above assumption is based on the observation that the Γ_s in Fig. 3 changes from the Γ_s of the (II) orientation to the Γ_s of the (III) orientation with a decrease in the surface charge density.

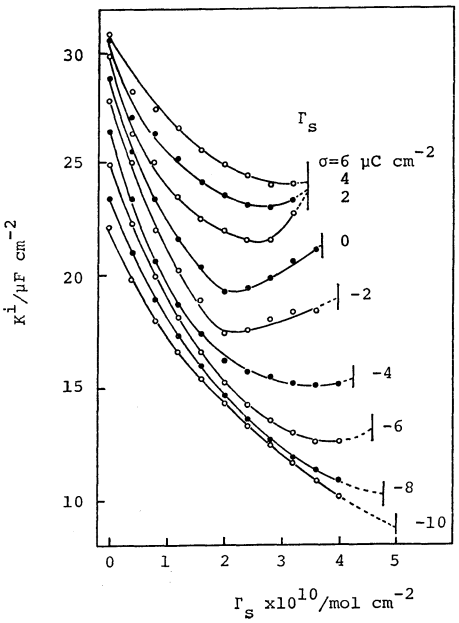

Fig.10. Plot of the integral inner-layer capacity against the surface excess at different surface charge density. Charge density is indicated by each line. Short vertical line represents Γ_s at each surface charge density.

The P_1, ε_1, and K_1^i values finally evaluated are summarized in Table 2, along with K_0^i and $K_0^{i(\text{ion})}$. The result with respect to P_1 indicates that the angles of the C=O bond axis to the electrode surface are about 25°, 90°, and 30° for the (I), (II), and (III) orientations respectively. The models in Fig. 9 were approximately confirmed by the evaluation of the dipole moment of TMU. Since the P_1 for the (I) orientation is almost constant, irrespective of the charge density, it seems most likely that the variation in the interaction parameter with the charge density is not caused by a slight change in the orientation, but by an interaction with neighboring water structure. It was further observed that the P_1 for the (II) orientation was almost the same as that measured on the basis of the polarization phenomena in the bulk of the solution, 11.6×10^{-30} C m.[3]

In summary, the adsorption behavior of TMU can be interpreted as follows. The principal orientation of the TMU adsorbed from lower concentrations is the (I) orientation, which is governed by an interaction with the neighboring water structure. With an increase in the surface excess, however, this orientation changes into the (II) or (III) orientation, depending on the charge sign of the electrode. The orientation at full coverage in the region of $0\geqslant\sigma\geqslant-8$ μC cm^{-2} is a mixture of (II) and (III). The (I) orientation was quite similar to that of urea.[5]

Since the dipole moment of TMU acts along the C$^+$–O$^-$ bond axis, the observed orientations deviate from those expected from the polarity. For example, the (II) orientation is the most probable orientation at a negative electric field, but it was not observed. Such an deviation from the expectation is often observed,[1,2,36,37] however, and this suggests that the electric field is effective for a short-range interaction, but not for a long-range interaction. The polarity of TMU was not an important factor governing the adsorption behavior. The scarcity of the positive charge on N atoms attributable to a weak conjugation is con-

Table 2. Various inner-layer parameters at saturation with TMU and water

σ/μC cm^{-2}	6	4	2	0	−2	−4	−6	−8	−10
K_0^i/μF cm^{-2}	30.8	30.5	29.8	28.8	27.8	26.4	24.9	23.4	22.1
$K_0^{i(\text{ion})}$/μF cm^{-2}	24.7	24.5	24.1	23.4	22.7	21.8	20.8	19.7	18.8
(I) Constant orientation with $\Gamma_s=3.45\times10^{-10}$ mol cm^{-2}									
K_1^i/μF cm^{-2}	—	—	—	14.5	13.2	12.2	11.8	11.5	11.3
$\varepsilon_1\times10^{11}$/F m^{-1}	—	—	—	8.4	7.6	7.1	6.8	6.6	6.6
$P_1\times10^{30}$/C m	—	—	—	5.5	5.0	5.0	5.3	5.3	5.5
(II) Variable orientation with $\Gamma_s=(3.5—5.0)\times10^{-10}$ mol cm^{-2}									
$\Gamma_s\times10^{10}$/mol cm^{-2}	3.5	3.5	3.5	3.7	4.0	4.3	4.6	4.8	5.0
K_1^i/μF cm^{-2}	24.2	24.0	23.4	21.3	18.6	15.4	13.2	10.2	8.8
$\varepsilon_1\times10^{11}$/F m^{-1}	14.0	13.8	13.6	12.5	11.1	9.3	8.1	6.3	5.5
$P_1\times10^{30}$/C m	11.9	11.5	11.5	11.1	10.6	9.3	8.3	7.5	6.1

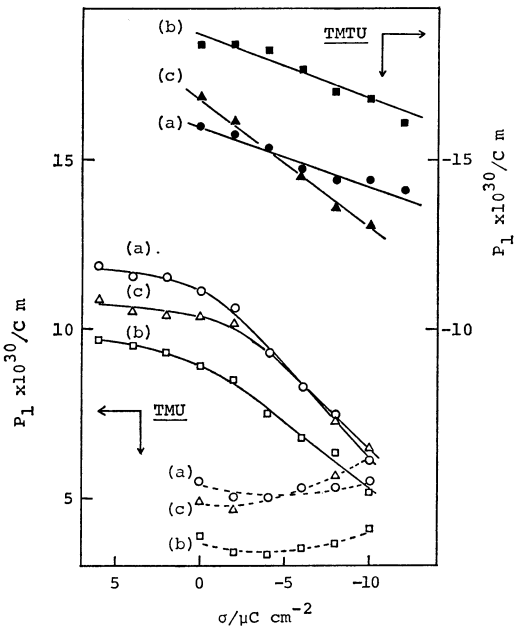

Fig.11. Comparison of P_1 estimated from different water-adsorption models.
(a) B-H model, (b) T-model, and (c) D-F model. Open and closed symbols correspond to TMU and TMTU, respectively.

sidered to be a main cause of the observed adsorption behavior, namely, an attractive interaction between electrons on N atoms and the positive charge on the electrode, and a repulsive interaction at a very negative charge density in addition to the lateral attractive interaction among TMU dipoles in the adsorption layer.

P_1 Evaluated from Different Water-adsorption Models. It is important to use an appropriate Δg^{w}_{dipole} value for the evaluation of P_1 using Eq. 4; it is also important to know the precise orientation state of the adsorbate on the molecular level. Aside from the different ideas contained in the water-adsorption models, as has already been mentioned, the values of Δg^{w}_{dipole} are different among the models. Figure 11 shows the P_1 values of TMU evaluated using the B-H model, the D-F model, and the T model. The results with TMTU[1)] are also plotted in the same figure. A positive (negative) value of P_1 means an orientation with the positive (negative) end of the dipole toward the electrode. In general, the dipole moment of an organic molecule adsorbed around $\sigma=0$ μC cm^{-2} seems to be nearly the same as that measured on the basis of the polarization phenomena in the bulk of the solution. In this sense, the B-H model seems to give reasonable P_1 values for TMU and TMTU.

The difference in P_1 value among the three models was not so large as was expected from the difference in the Δg^{w}_{dipole}, probably because of a compensation action due to $K_0^{i(ion)}$. Strictly speaking, however, the following features are recognized. The way of the variation in P_1 with the charge density between the B-H model and the T model is almost the same, but the values of P_1 are different. On the contrary, the way of the variation in P_1 with the charge density between the B-H model and the D-F model is somewhat different, but the values of P_1 are approximately the same.

References

1) O. Ikeda, H. Jimbo, and H. Tamura, *J. Electroanal. Chem.*, **137**, 127 (1982).
2) R. Parsons, *Proc. R. Soc. London, Ser. A*, **261**, 79 (1961).
3) Cl. Béguin and T. Gäumann, *Helv. Chim. Acta*, **45**, 1971 (1958).
4) S. Trasatti, *J. Electroanal. Chem.*, **53**, 335 (1974).
5) R. Parsons, R. Peat, and R. M. Reeves, *J. Electroanal. Chem.*, **62**, 151 (1975).
6) R. Parsons and P. C. Symons, *Trans. Faraday Soc.*, **64**, 1077 (1968).
7) S. Trasatti, "Modern Aspects of Electrochemistry," Plenum Press, New York (1979), Vol. 13, p. 81.
8) J. O'M Bockris and M. A. Habib, *Electrochim. Acta*, **22**, 41 (1977).
9) S. Trasatti, *J. Electroanal. Chem.*, **64**, 128 (1975).
10) B. B. Damaskin and A. N. Frumkin, *Electrochim. Acta*, **19**, 173 (1974).
11) G. J. Hills and R. Payne, *Trans. Faraday Soc.*, **61**, 316 (1965).
12) D. C. Grahame, E. M. Coffin, J. P. Cummings, and M. A. Poth, *J. Am. Chem. Soc.*, **74**, 1207 (1952).
13) D. J. Schiffrin, *J. Electroanal. Chem.*, **23**, 168 (1969).
14) A. De Battisti and S. Trasatti, *J. Electroanal. Chem.*, **54**, 1 (1974).
15) D. M. Mohilner and H. Nakadomari, *J. Phys. Chem.*, **77**, 1594 (1973).
16) D. M. Mohilner, L. W. Browman, S. J. Freeland, and H. Nakadomari, *J. Electrochem. Soc.*, **120**, 1658 (1973).
17) B. B. Damaskin, O. A. Petrii, and V. V. Batrakov, "Adsorption of Organic Compounds on Electrodes," Plenum Press, New York (1971), p. 84.
18) R. Parsons, *Trans. Faraday Soc.*, **51**, 1518 (1955).
19) P. Delahay, "Double Layer and Electrode Kinetics," Interscience, New York (1965), p. 23.
20) D. C. Grahame, *Chem. Rev.*, **41**, 441 (1947).
21) A. N. Frumkin, B. B. Damaskin, and A. A. Survila, *J. Electroanal. Chem.*, **16**, 493 (1968).
22) B. E. Conway, H. P. Dhar, and S. Gottesfeld, *J. Colloid Interface Sci.*, **43**, 303 (1973).
23) S. Trasatti, *J. Electroanal. Chem.*, **28**, 257 (1970).
24) R. Parsons, *Trans. Faraday Soc.*, **55**, 999 (1959).
25) F. Pulidori, G. Borghesani, R. Pedriali, A. De Battisti, and S. Trasatti, *J. Chem. Soc., Faraday Trans. 1*, **74**, 79 (1978).
26) J. O'M Bockris, E. Gileadi, and K. Müller, *Electrochim. Acta*, **12**, 1301 (1967).
27) J. E. Worsham, Jr., H. A. Levy, and S. W. Peterson, *Acta Crystallogr.*, **10**, 319 (1957).
28) R. J. Niedzielski, R. S. Drago, and R. L. Middaugh, *J. Am. Chem. Soc.*, **86**, 1694 (1964).
29) L. Fernholt, S. Samdal, and R. Seip, *J. Mol. Struct.*, **72**, 217 (1981).
30) F. A. L. Anet and M. Ghiaci, *J. Am. Chem. Soc.*, **101**, 6857 (1979).
31) A. Luttrinhaus and J. Grohman, *Z. Naturforsch., B*, **10**, 365 (1955).
32) J. D. Swalen and C. C. Costain, *J. Chem. Phys.*, **31**, 1562 (1959).
33) M. Schafer and C. Curran, *Inorg. Chem.*, **5**, 265 (1966).
34) B. B. Damaskin and A. N. Frumkin, *J. Electroanal. Chem.*, **34**, 191 (1972).
35) S. Trasatti, *J. Electroanal. Chem.*, **64**, 128 (1973).
36) L. M. Baugh and R. Parsons, *J. Electroanal. Chem.*, **41**, 311 (1973).
37) G. J. Hills, D. J. Schiffrin, and T. Solomon, *J. Electroanal. Chem.*, **41**, 41 (1973).